# The Partial Oxidation of Ethane over a $B_2O_3$-$Al_2O_3$ Catalyst

Yasushi MURAKAMI, Kiyoshi OTSUKA,* Yuji WADA, and Akira MORIKAWA
Department of Chemical Engineering, Tokyo Institute of Technology, Ookayama, Meguro-ku, Tokyo 152
(Received September 2, 1989)

The catalytic activities were examined for the partial oxidation of ethane over various metal oxides. $B_2O_3$(30wt%)-added $Al_2O_3$ showed the highest catalytic activity in the formation of acetaldehyde (yield: 1.03%) and ethylene (14.6%). Ethylene and acetaldehyde are assumed to be formed via a common reaction intermediate because of the similarity in their kinetic behavior and the similar activation-energy values observed. The second-order dependence of the formation rates for the two products on the pressure of ethane suggests that the two molecules of ethane participate in the formation of the intermediate in the chain reaction mechanism proposed. The active site for the formation of acetaldehyde from the intermediate is suggested to be a highly dispersed boron electron-donated from alumina, but that for ethylene must be different from that of acetaldehyde.

The one-step conversion of light alkanes to their partial oxidation products, such as alkenes, alcohols, aldehydes, or acids, is of importance for effective use of alkanes contained in natural gas. There have been some reports on the conversion of ethane to ethylene through oxidative dehydrogenation with oxygen gas on Mo-V-Nb/$Al_2O_3$[1] and $SnO_2$-$P_2O_5$.[2] However, the conversion of ethane to $C_2$-oxygenates was successful on Mo/$SiO_2$[3,4] and Co/MgO[5] only when $N_2O$ was used as the oxidant. It is necessary to develop catalysts on which the conversion of ethane to $C_2$-oxygenates with oxygen gas proceeds effectively.

We have found that $B_2O_3$-$Al_2O_3$ is an active and selective catalyst for the partial oxidation of ethane to ethylene and acetaldehyde using oxygen.[6] Boron-based catalysts are also effective for the formation of oxygenates by means of the partial oxidation of methane[7,8] and propane.[9] These catalysts are characterized by a lack of the redox property, in contrast with the molybdenum oxide-based catalysts, which have been investigated most extensively for the partial oxidation of light alkanes to their oxygenates.[4,10-14] A mechanism involving the redox cycle of the molybdenum ion has been proposed for this system.[4,10] Since the oxidation state of boron cannot change under these reaction conditions, the mechanism of the partial oxidation of alkanes over boron oxide-based catalysts must be quite different from that proposed for the molybdenum oxide-based catalysts.

In this paper, the state of boron oxide on $Al_2O_3$ and the reaction kinetics over the $B_2O_3$-$Al_2O_3$ catalyst will be investigated. The role of boron oxide will be discussed, and a reaction mechanism will be proposed.

## Experimental

The metal oxides used were purchased from the Wako Chemical Co., while the alumina used as the reference catalyst, JRC-ALO-2, was supplied by the Catalysis Society of Japan. The boron oxide supported on various oxides was prepared by an impregnation method with metal oxide powders and an aqueous solution of boric acid. These catalysts were calcined in air at 873 K. The contents of boron oxide in the catalysts are denoted in the parentheses, for example, the $Al_2O_3$ with 30 wt% $B_2O_3$ added as $B_2O_3$(30)-$Al_2O_3$. A conventional gas flow system with a fixed-bed reactor made of quartz was used in the experiments.

Ethane and oxygen gases were fed with a helium-gas carrier to the catalyst under atmospheric pressure. The reaction temperature for the test of the catalysts was 823 K. The products were analyzed by means of gas chromatography. The selectivities and the yields of the products were expressed on the basis of the ethane converted into each product. The X-ray photoelectron spectra (XPS) were obtained using a spectrometer (Surface Science Laboratory, SSX-100) with monochrometric alumina $K\alpha$ radiation (1486.6 eV); the charge compensation was effected by means of an electron flood gun. The spectra were calibrated against the carbon 1s line (285.0 eV) attributable to the carbon deposit on the surface.

## Results

**Catalytic Activities of Various Metal Oxides.** The catalytic activities were examined for the oxidation of ethane over the oxides of B, Mg, Al, Si, Ca, Ti, V, Cr, Mn, Fe, Co, Ni, Cu, Zn, Ga, Sr, Y, Zr, Nb, Mo, Cd, In, Sn, Sb, Te, Ba, La, Ce, W, Pb, and Bi. Oxygenated hydrocarbons were formed only over the oxides of B, Al, and Si. $B_2O_3$ was more selective for the formations of ethylene and acetaldehyde than were $Al_2O_3$ and $SiO_2$, on which CO and $CO_2$ were mainly produced (see Table 1). However, the yield of acetaldehyde for $B_2O_3$ was low, i.e., less than 0.1%.

The catalytic activities of the boron oxide supported on various metal oxides were tested (Table 1). $B_2O_3$-$Al_2O_3$, $B_2O_3$-MgO, $B_2O_3$-$La_2O_3$, and $B_2O_3$-$P_2O_5$ were effective catalysts. They were more active and selective for the formation of acetaldehyde than was the $B_2O_3$ catalyst without supports. The yields of ethylene and acetaldehyde for $B_2O_3$-$Al_2O_3$ were the highest among those for the four catalysts. $B_2O_3$-$SiO_2$ and $B_2O_3$-$TiO_2$ were also selective for the partial oxidation, but they were less active. On the other hand, deep oxidation mainly proceeded over $B_2O_3$-CaO and $B_2O_3$-ZnO.

The stability of $B_2O_3$(30)-$Al_2O_3$, the most active

Table 1. Partial Oxidation of Ethane over Various Oxide Catalysts at 823 K

| Catalyst | Conv. /% | Selectivity /% | | | | | Yield /% | |
|---|---|---|---|---|---|---|---|---|
| | | $C_2H_4$ | $CH_3CHO$ | CO | $CO_2$ | $CH_4$ | $C_2H_4$ | $CH_3CHO$ |
| None | 0.2 | 89.0 | 0 | 0 | 11.0 | 0 | 0.2 | 0 |
| $B_2O_3$ | 3.8 | 97.1 | 2.6 | 0 | 0.3 | 0 | 3.7 | 0.10 |
| $Al_2O_3$ | 22.3 | 12.4 | 0.2 | 55.3 | 32.0 | 0 | 2.8 | 0.04 |
| $SiO_2$ | 4.4 | 37.4 | 1.2 | 54.6 | 6.8 | 0 | 1.6 | 0.06 |
| $B_2O_3$-$Al_2O_3$[a] | 38.0 | 58.0 | 2.7 | 31.0 | 1.6 | 4.9 | 14.6 | 1.03 |
| $B_2O_3$-$La_2O_3$[a] | 5.7 | 82.6 | 6.9 | 8.2 | 1.3 | 1.0 | 4.7 | 0.39 |
| $B_2O_3$-MgO[a] | 4.6 | 80.0 | 7.7 | 8.5 | 2.8 | 1.0 | 3.7 | 0.35 |
| $B_2O_3$-$P_2O_5$[a] | 2.1 | 89.7 | 9.4 | 0 | 0.9 | 0 | 1.9 | 0.20 |
| $B_2O_3$-$SiO_2$[a] | 3.6 | 96.0 | 2.5 | 0.3 | 0.3 | 0.5 | 3.5 | 0.09 |
| $B_2O_3$-$TiO_2$[a] | 0.4 | 98.0 | 2.0 | 0 | 0 | 0 | 0.4 | 0.01 |
| $B_2O_3$-CaO[a] | 5.8 | 30.2 | 0.3 | 30.3 | 39.0 | 0.2 | 1.7 | 0.02 |
| $B_2O_3$-ZnO[a] | 35.0 | 40.6 | 0 | 2.7 | 56.5 | 0.2 | 14.4 | 0 |
| $B_2O_3$-$Al_2O_3$[b] | 21.9 | 12.5 | 0.2 | 55.5 | 31.8 | 0 | 2.8 | 0.04 |

Reaction temperature=823 K, weight of catalyst=0.5 g, Flow rate=50 ml $min^{-1}$, $P(C_2H_6)$=20 kPa, $P(O_2)$=20 kPa. a) The content of $B_2O_3$ is 30 wt%. b) After washing with distilled water.

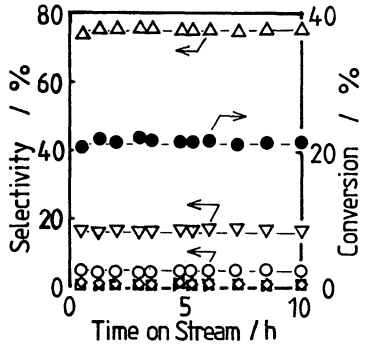


Fig. 1. Stability in catalytic activity of $B_2O_3$(30)-$Al_2O_3$ with time on stream. $C_2H_6$ conversion (●), selectivity of $C_2H_4$ (△), acetaldehyde (○), CO (▽), $CO_2$ (□), and $CH_4$ (◇). Reaction temperature=823 K, weight of catalyst=0.5 g, flow rate=50 ml $min^{-1}$, $P(C_2H_6)$=10 kPa, $P(O_2)$=10 kPa.

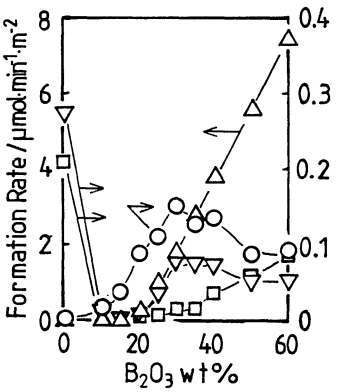


Fig. 2. Formation rates of productions as function of the content of $B_2O_3$. $C_2H_4$ (△), acetaldehyde (○), CO (▽), and $CO_2$ (□). Reaction temtperature=823 K, weight of catalyst=0.05 g, flow rate=100 ml $min^{-1}$, $P(C_2H_6)$=10 kPa, $P(O_2)$=10 kPa.

catalyst, in the catalytic activity and selectivity with the time on a stream is shown in Fig. 1. The conversion of ethane and the selectivities for all the products were constant throughout the 10 hours of the reaction.

The formation rates of the products over a unit of surface area of $B_2O_3$-$Al_2O_3$ with the various contents of $B_2O_3$ are shown in Fig. 2. Though ethane was highly converted over pure alumina, the main products were CO and $CO_2$. When 10 wt% of $B_2O_3$ was added, the formations of CO and $CO_2$ were drastically suppressed. However, the rate of the formation of ethylene was increased linearly by the addition of boron oxide above 20 wt%. On the other hand, the rate of acetaldehyde formation began to increase at 15 wt% and showed a maximum value at 30 wt%. The selectivities for the formation of acetaldehyde (31.1% and 25.0% on $B_2O_3$(15)-$Al_2O_3$ and $B_2O_3$(20)-$Al_2O_3$ respectively) were considerably higher than those observed for pure $B_2O_3$ in Table 1 (2.6%). The total selectivity for the partial oxidation products ($C_2H_4$+$CH_3CHO$) at a $B_2O_3$ content above 20 wt% was greater than 95%.

**Characterization of $B_2O_3$-$Al_2O_3$.** The XRD spectra of $B_2O_3$-$Al_2O_3$ with various contents of $B_2O_3$ are shown in Fig. 3. The XRD pattern attributed to crystalline $B_2O_3$ was observed for the $B_2O_3$-$Al_2O_3$ containing more than 20 wt% of $B_2O_3$, and the intensities of the diffraction in the spectra increased with an increase in the content of $B_2O_3$. There was no peak showing the formation of mixed oxides between $B_2O_3$ and $Al_2O_3$.

The surface areas of the catalysts with various contents of $B_2O_3$ are shown in Fig. 4. The area was significantly lowered above a 20 wt% $B_2O_3$ content, with a coincident growth of crystalline $B_2O_3$ observed in the XRD spectra. Therefore, this decrease in the surface area is probably due to the plugging of the pores in alumina by agglomerates of $B_2O_3$. This assumption was supported by the observation that the

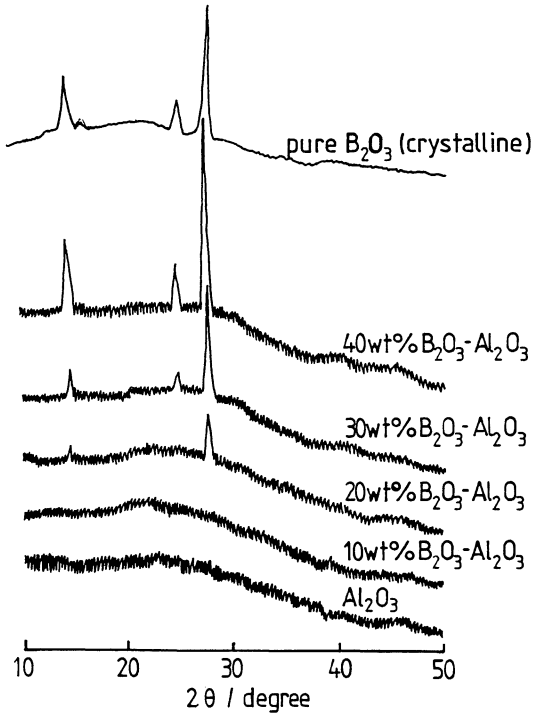


Fig. 3. XRD spectra of $B_2O_3$-$Al_2O_3$ with various contents of $B_2O_3$.

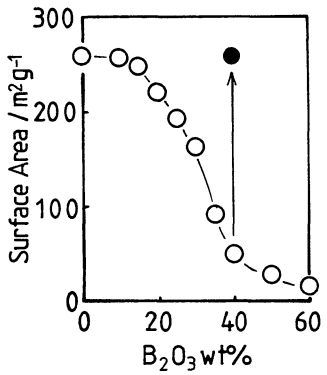


Fig. 4. Surface areas of $B_2O_3$-$Al_2O_3$ with various contents of $B_2O_3$. After washing with distilled water (●).

surface area of the $B_2O_3(40)$-$Al_2O_3$, 48 $m^2g^{-1}$, was restored to the original value of pure alumina, i.e., 258 $m^2g^{-1}$, after washing with distilled water at room temperature (as is indicated by the arrow in Fig. 4). The catalytic activity and selectivity after the washing treatment became comparable to those observed over alumina (see Table 1).

The X-ray photoelectron spectra of $B_2O_3$-$Al_2O_3$ were also measured. An asymmetric spectrum was observed for the spectra of the boron 1s electrons, as is shown in Fig. 5, with a solid curve for each sample. The asymmetric spectrum for each sample was decomposed into the main and the shoulder peaks. The binding energy of the shoulder peak was 189.7 eV, while that of the main peak was 192.2 eV (see Table 2). Tavadze et al. have observed the XPS spectra of $B_2O_3$ supported on silica.[15] They have also reported asymmetric spectra and have attributed the main peak to a crystalline $B_2O_3$. The shoulder peak has been attributed to the oxide of a cluster type consisting of a lower oxidation state of boron than that in a pure $B_2O_3$. With reference to this suggestion, the shoulder peak observed at 189.7 eV for $B_2O_3$-$Al_2O_3$ in our work can be attributed to the boron oxide of a cluster type described above. While the area of the main peak increased monotonously with the increase in the amount of $B_2O_3$, that of the shoulder peak showed a maximum at 30 wt% of $B_2O_3$ (see Table 2). The latter type of $B_2O_3$, showing a lower oxidation state of boron, could be formed on electron-donating sites on the surface of alumina, e.g., basic sites. The observation that the area of the XPS peak at the lower binding

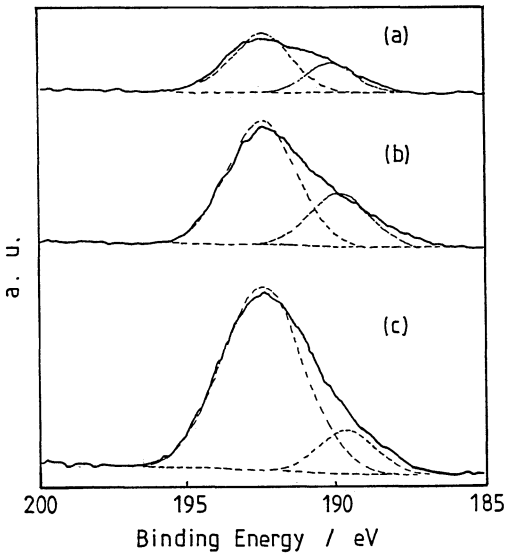


Fig. 5. XPS spectra in B(1s) electrons with $B_2O_3(10)$-$Al_2O_3$ (a), $B_2O_3(30)$-$Al_2O_3$ (b), and $B_2O_3(50)$-$Al_2O_3$ (c).

Table 2. Binding Energy in B(1s) Electrons and Boron Contents by XPS Spectra

| | Binding energy/eV (Area) | B/(Al+B)/mol% | |
|---|---|---|---|
| | | Surface | Overall[a] |
| $B_2O_3(10)$-$Al_2O_3$ | 192.3 (1883), 189.9 ( 901) | 29.3 | 14.0 |
| $B_2O_3(30)$-$Al_2O_3$ | 192.2 (3687), 189.7 (1502) | 50.9 | 38.5 |
| $B_2O_3(50)$-$Al_2O_3$ | 192.2 (5300), 189.4 ( 935) | 70.3 | 59.4 |

a) Calculated from the compositions in the preparation.

energy decreased above 30 wt% of the $B_2O_3$ (Table 1) must be ascribed to the growth of the crystalline $B_2O_3$ over the cluster-type $B_2O_3$, which has been generated on the basic sites of alumina.

The surface compositions of the catalysts estimated from the spectra are listed on Table 2. The ratios of boron were higher than those calculated from the compositions adjusted in the preparation of the samples, indicating that most of the boron added deposits on the alumina surface. This is natural, since the XRD spectra did not show any bulk compound oxide between $B_2O_3$ and $Al_2O_3$. Moreover, the decrease in the surface area of the samples with the rise in the content of $B_2O_3$ (Fig. 4) supports the deposit of crystalline $B_2O_3$ on the surface of alumina.

**Kinetic Studies.** Figure 6 shows the conversion of ethane and the yields of the products as functions of the *W/F* ratio. The conversion of ethane was increased linearly with the increase in the *W/F*. The yield of ethylene was proportional to the *W/F*. Though acetaldehyde was produced at a short contact time, the increase in the yield of acetaldehyde was suppressed, while the formations of CO, $CO_2$, and methane were accelerated, at a longer contact time. This suggests that CO, $CO_2$, and methane were formed through either the decomposition or the further oxidation of acetaldehyde produced.

The products of the reaction of ethane over $B_2O_3(30)$-$Al_2O_3$, i.e., ethylene and acetaldehyde, were fed over the catalyst with oxygen gas. These experiments were carried out under partial pressures of ethylene and acetaldehyde similar to those observed in the ethane oxidation. No acetaldehyde was formed from ethylene at 1.3 kPa. Acetaldehyde with a partial pressure of 0.14 kPa was converted to CO, $CO_2$, and methane, with a 65% conversion, at 823 K. These results support the suggestion that CO, $CO_2$, and methane are formed from acetaldehyde. Moreover, the results show that acetaldehyde and ethylene are formed in parallel from ethane.

The dependence of the catalytic activity on the reaction temperatures over $B_2O_3$-$Al_2O_3$ was also investigated. The logarithms of the formation rates of ethylene and acetaldehyde were plotted against the reciprocal of the reaction temperatures (see Fig. 7). The real formation rate of acetaldehyde was calculated from the sum of the formation rates of acetaldehyde, CO, $CO_2$, and methane, as the latter three are formed from acetaldehyde. The rates for the latter three were

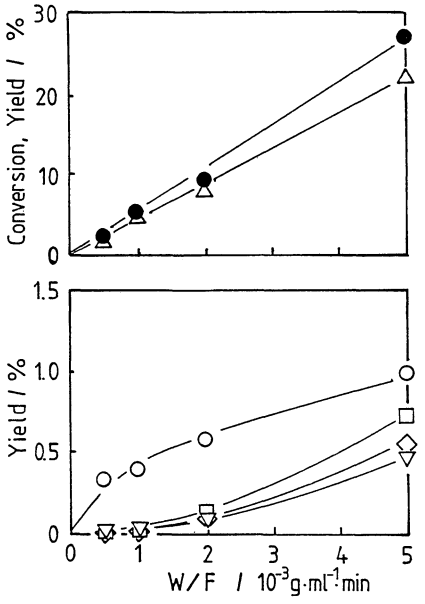


Fig. 6. Effect of contact time on the conversion of ethane and the formation of products. $C_2H_6$ conversion (●), selectivity of $C_2H_4$ (△), acetaldehyde (○), CO (▽), $CO_2$ (□), and $CH_4$ (◇). Reaction temperature=823 K, weight of catalyst=0.05 g, flow rate=50 ml $min^{-1}$, $P(C_2H_6)$=10 kPa, $P(O_2)$=10 kPa.

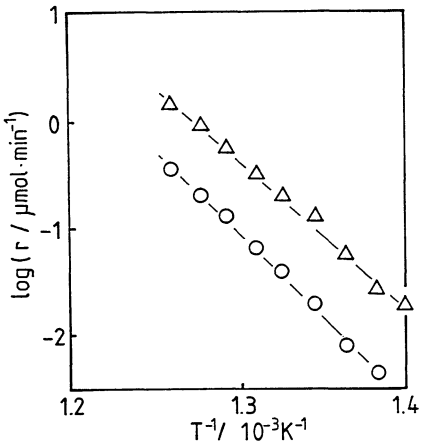


Fig. 7. Effect of reaction temperatures on partial oxidation of ethane over $B_2O_3(30)$-$Al_2O_3$. Ethylene (△), and acetaldehyde (○). Weight of catalyst=0.05 g, flow rate=100 ml $min^{-1}$, $P(C_2H_6)$=20 kPa, $P(O_2)$=20 kPa.

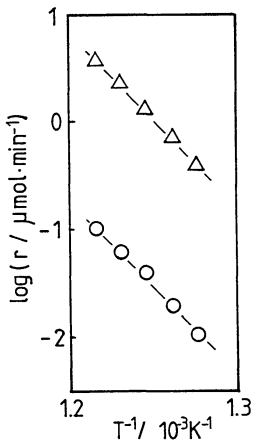


Fig. 8. Effect of reaction temperatures on partial oxidation of ethane over $B_2O_3(30)$-$SiO_2$. Ethylene (△), and acetaldehyde (○). Weight of catalyst= 0.05 g, flow rate=50 ml $min^{-1}$, $P(C_2H_6)$=20 kPa, $P(O_2)$=20 kPa.

evaluated on the basis of $C_2$. The formation rate of acetaldehyde to be described hereafter is the one defined above. The apparent activation energies for the formations of ethylene and acetaldehyde over $B_2O_3$-$Al_2O_3$ were 310 and 280 kJ mol$^{-1}$ respectively.

The activation energies for the formations of ethylene and acetaldehyde over $B_2O_3$-$SiO_2$ were similarly estimated from the plot of $\log r$ vs. $1/T$ (Fig. 8). These values were 310 and 290 kJ mol$^{-1}$ respectively, the same as those observed for the $B_2O_3$-$Al_2O_3$ within the limits of experimental error (±10 kJ mol$^{-1}$).

Figure 9 shows the relationship between the formation rates of ethylene and acetaldehyde and the square of the pressure of ethane for $B_2O_3(30)$-$Al_2O_3$. The straight lines in Fig. 9 indicate that the formation rates of both ethylene and acetaldehyde show a second-order dependence on the pressure of ethane.

A linear relationship was observed when the pressure of oxygen divided by the formation rates of ethylene and acetaldehyde was plotted against the pressure of oxygen (see Fig. 10). The results in Fig. 10 show

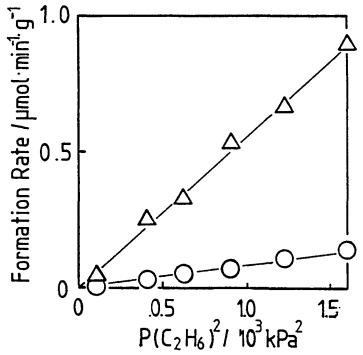


Fig. 9. Effect of the pressure of ethane on partial oxidation of ethane over $B_2O_3(30)$-$Al_2O_3$. Ethylene (△), and acetaldehyde (○). Reaction temperature=773 K, weight of catalyst=0.05 g, flow rate=100 ml min$^{-1}$, $P(O_2)$=10 kPa.

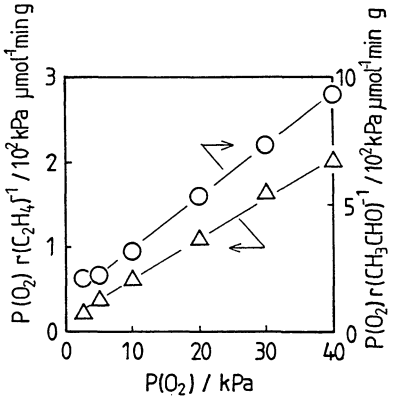


Fig. 10. Effect of the pressure of oxygen on partial oxidation of ethane over $B_2O_3(30)$-$Al_2O_3$. Ethylene (△), and acetaldehyde (○). Reaction temperature=773 K, weight of catalyst=0.05 g, flow rate=100 ml$^{-1}$, $P(C_2H_6)$=20 kPa.

that the dependence of each formation rate on the pressure of oxygen can be expressed by the following equation:

$$r = \frac{A\,P(O_2)}{1 + B\,P(O_2)}.$$

This observation suggests that the formation rates are proportional to the concentration of oxygen which is molecularly adsorbed on the surface.

## Discussion

As has been described earlier, $B_2O_3$-$Al_2O_3$, $B_2O_3$-MgO, $B_2O_3$-$La_2O_3$, and $B_2O_3$-$P_2O_5$ are selective catalysts for the partial oxidation of ethane. Among these catalysts, $B_2O_3(30)$-$Al_2O_3$ showed the highest catalytic activity in the formations of acetaldehyde (yield 1.03%) and ethylene (14.6%). This catalyst was stable under the reaction conditions shown in Fig. 1. Iwamoto et al.[3] and Mendelovici and Lunsford[4] have reported that the yields of acetaldehyde are 1.63% and 1.37% respectively for the partial oxidation of ethane at 823 K over $MoO_3/SiO_2$ with $N_2O$ as the oxidant. When we examined the partial oxidation of ethane over the $MoO_3$ (7 wt%)-$SiO_2$ catalyst, using $O_2$ as the oxidant under the conditions shown in Table 2, the yield of ethylene (0.9%) was even smaller than that for $SiO_2$ (1.6%), while the yield of acetaldehyde (0.07%) was comparable to that for $SiO_2$ (0.06%). Thus, when we use $O_2$ as the oxidant, $MoO_3/SiO_2$ is not an effective catalyst in partial oxidation of ethane. In contrast, the yield of acetaldehyde observed for the $B_2O_3(30)$-$Al_2O_3$, using $O_2$ as the oxidant, is comparable to those over $MoO_3/SiO_2$ when $N_2O$ is used.

**Active Sites.** The activation energies for the formations of ethylene and acetaldehyde over $B_2O_3$-$Al_2O_3$ were close to those observed for $B_2O_3$-$SiO_2$. This suggests that common active sites in the two catalysts, i.e., a crystalline $B_2O_3$ and a cluster type $B_2O_3$ may be responsible for the formations of the products. At a $B_2O_3$ content greater than that of 30 wt% shown in Fig. 2, the rate of ethylene formation or the rate of conversion of ethane over a unit of surface area increased linearly with a rise in the amount of $B_2O_3$. Above this content of $B_2O_3$, most of the boron added to $Al_2O_3$ must be in the state of crystalline $B_2O_3$ as has been described earlier (see Fig. 3 and Table 2). Therefore, the crystalline $B_2O_3$ must be responsible for the initial activation of ethane (C-H bond cleavage).

The rate of acetaldehyde formation over a unit of surface area increased with the amount of $B_2O_3$ in the range of content between 10 to 30 wt%. However, it decreased above 30 wt%, where the maximum was reached. Although the formation of acetaldehyde requires the participation of crystalline $B_2O_3$ in the initial activation of ethane, different active sites must be responsible for its further oxidation to acetaldehyde.

Boron oxide added over the alumina at a content

below 10 wt% showed no XRD pattern, indicating that $B_2O_3$ was highly dispersed. This highly dispersed $B_2O_3$ could suppress the formations of CO and $CO_2$ observed over alumina (Fig. 2). The active site on alumina for deep oxidation must be poisoned by a small amount of boron oxide (ca. 10 wt%). Assuming that the crystal structure of $B_2O_3$ is cubic, the calculated amount of the monolayer $B_2O_3$ over alumina (265 $m^2 g^{-1}$) is 0.003 mol per gram of alumina, which may be evaluated as equivalent to 19 wt% of $B_2O_3$. Thus, the amount of $B_2O_3$ for a monolayer over the alumina is adequate to completely poison the deep oxidation sites on the alumina.

The interaction between boron and alumina was proved by the XPS measurements in Fig. 5. The area of the XPS peak corresponding to the cluster type of $B_2O_3$ of a lower oxidation state showed a maximum at the amount of $B_2O_3$ of 30 wt% (Table 2). The results in Fig. 2 show that the maximum yield of acetaldehyde was observed at this content of $B_2O_3$, suggesting that the boron-oxide cluster is the active site for the formation of acetaldehyde.

**Reaction Mechanism.** As has been described in the Results section, CO, $CO_2$, and methane are formed from acetaldehyde. Acetaldehyde is formed not via ethylene but directly from ethane and is successively decomposed to CO, $CO_2$, and methane. The similar kinetics observed for the formations of ethylene and acetaldehyde (Figs. 7, 9, and 10) suggest a reaction path through a common intermediate to the two products. The network of the reactions may be written as follows:

$$C_2H_6 \rightarrow \text{Intermediate} \begin{cases} \rightarrow C_2H_4 \\ \rightarrow CH_3CHO \rightarrow \begin{matrix} CO \\ CO_2 \\ CH_4 \end{matrix} \end{cases}$$

The linear increase in the yield of $C_2H_4$ and the sum of $CH_3CHO$, CO, $CO_2$ and $CH_4$ with a rise in the $W/F$ ratio in Fig. 6 suggest parallel formations of $C_2H_4$ and $CH_3CHO$ through a common reaction intermediate. The similar rate equations observed for the formation of ethylene and acetaldehyde (Figs. 9 and 10) support the presence of the common intermediate shown in the network, as will be described later.

The second-order dependence of the formation rates on the pressure of ethane (Fig. 9) suggests that the two molecules of ethane participate in the reaction mechanism. A tentative chain reaction mechanism on the surface is proposed as follows. The second molecule of ethane may participate in the chain propagation after the activation of ethane.

$$C_2H_6 + O^* \xrightarrow{k_1} C_2H_5 + OH \quad (1)$$

$$C_2H_5 + O_2 \underset{k_{-2}}{\overset{k_2}{\rightleftharpoons}} C_2H_5O_2 \quad (2)$$

$$C_2H_5O_2 + C_2H_6 \xrightarrow{k_3} C_2H_5OOH + C_2H_5 \quad (3)$$

$$C_2H_5 + O^* \xrightarrow{k_4} C_2H_4 + OH \quad (4)$$

Ethane is converted to an ethyl radical through the abstraction of hydrogen by adsorbed active oxygen species, $O^*$, on crystalline $B_2O_3$ (Eq. 1) (activation of $C_2H_6$). $O^*$ also abstracts the hydrogen of the ethyl radical to give ethylene (Eq. 4) (termination). Here, $O^*$ could be $O^-$, $O_2^-$, or $O_2^{2-}$ on the crystalline $B_2O_3$. However, no information about the nature of $O^*$ has yet been obtained. The addition of adsorbed diatomic oxygen to the ethyl radical forms an ethylperoxyl radical (Eq. 2). The forward and backward reactions in Eq. 2 must be in equilibrium. Then the ethylperoxyl radical reacts with ethane, forming ethyl hydroperoxide and regenerating the ethyl radical. Reaction Steps 2 and 3 are similar to the mechanism of the autooxidation of ethane in the gas phase.[16,17] Ethyl hydroperoxide seems to decompose to ethylene or to acetaldehyde on the surface through the following steps, Steps 5 and 6:

$$C_2H_5OOH \xrightarrow{k_5} C_2H_4 + 1/2\ O_2 + H_2O \quad (5)$$

$$C_2H_5OOH \xrightarrow{k_6} CH_3CHO + H_2O \quad (6)$$

Bashkirov et al. found that the autooxidation of alkanes ($C_{12}$ to $C_{30}$) in the presence of $H_3BO_3$ or $B_2O_3$ gave the corresponding secondary alcohols with a high selectivity.[18] Broich and Grasemann suggested that the boric acids react with hydroperoxides to give boric esters selectively as follows:[19]

$$\begin{matrix} OH \\ | \\ -B-O- \end{matrix} + ROOH \rightarrow \begin{matrix} O^+H_2 \\ | \\ -B-O- \\ | \\ OOR \end{matrix} \rightarrow \begin{matrix} \\ \\ -B-O- \\ | \\ OR \end{matrix} + 1/2\ O_2 + H_2O$$

Although no alcohols were observed in our work, the formation of ethylene may proceed through a boric ester similar to that described above. The boric ester from the reaction of ethyl hydroperoxide with boron oxide could give ethylene instead of ethanol at higher temperatures. However, acetaldehyde (Step 6) could not be formed through boric ester, for different active sites must be responsible for the two reactions (Eqs. 5 and 6), as has been suggested above.

When we can neglect the participations of OH in chain propagations, the concentration of ethyl hydroperoxide can be derived on the basis of a steady-state approximation of the concentrations of the reaction intermediates, $C_2H_5$, $C_2H_5O_2$, and $C_2H_5OOH$, as follows:

$$[C_2H_5OOH] = \frac{k_1 k_2 k_3}{k_4(k_{-2}+k_3[C_2H_6])(k_5+k_6)} [C_2H_6]^2 [O_2] \quad (7)$$

The decomposition of the ethylperoxyl radical should be much faster than the reaction with ethane ($k_{-2} \gg k_3[C_2H_6]$). Let us assume that the concentration of oxygen adsorbed on the surface can be written by Langmuir's equation:

$$[O_2] = n_o \frac{K_o P(O_2)}{1+K_o P(O_2).}$$

where $n_o$ and $K_o$ are the number of adsorption sites

and the adsorption constant for oxygen respectively. On the other hand, the weak interaction between ethane and the surface leads to the linear relationship between the surface concentration and the pressure of ethane ($[C_2H_6]=n_e K_e P(C_2H_6)$). Therefore, the concentration of ethyl hydroperoxide can be represented by the following equation:

$$[C_2H_5OOH] \simeq K\, P(C_2H_6)^2 \frac{K_o\, P(O_2)}{1+K_o\, P(O_2)} \quad (8)$$

$$\text{where } k=\frac{k_1\, k_2\, k_3\, (n_e\, K_e)^2\, n_o}{k_4\, k_{-2}\, (k_5+k_6)}$$

The rate equations for the formations of ethylene and acetaldehyde can be set up as follows:

$$r(C_2H_4)=k_5[C_2H_5OOH]+k_4[C_2H_5][O^*] \quad (9)$$

$$r(CH_3CHO)=k_6[C_2H_5OOH] \quad (10)$$

The formation of ethylene directly from the ethyl radical with $O^*$ (Termination Step 4) should be much slower than that through ethyl hydroperoxide (Steps 2,3,5)($k_5[C_2H_5OOH] \gg k_4[C_2H_5][O^*]$). The substitutions of the concentration of ethyl hydroperoxide into Eqs. 9 and 10 with Eq. 8 yield the following equations:

$$r(C_2H_4) \simeq k_5\, k\, P(C_2H_6)^2 \frac{K_o\, P(O_2)}{1+K_o\, P(O_2)} \quad (11)$$

$$r(CH_3CHO) \simeq k_6 k\, P(C_2H_6)_2 \frac{K_o\, P(O_2)}{1+K_o\, P(O_2)} \quad (12)$$

These equations explain well the rate equations observed (Figs. 9 and 10).

The similar activation energies for the formation of ethylene and acetaldehyde observed in Fig. 7 can be explained by Eqs. 11 and 12 if the activation energies of Steps 5 and 6 are smaller than that of the initiation (Step 1). It seems reasonable that the C-H bond activation requires much more energy than those of Steps 2—6. The decompositions of unstable ethyl hydroperoxide (Steps 5 and 6) should have much lower activation energies than that of Step 1. The similar activation energies observed for $B_2O_3$-$Al_2O_3$ (Fig. 7) and $B_2O_3$-$SiO_2$ (Fig. 8) were natural, since the activation of ethane occurs on the same active sites, i.e., on the crystalline $B_2O_3$.

**The Role of Alumina.** The favorable carrier effect of alumina on boron oxide demonstrated in Table 1 was to enhance the conversion of ethane as well as the yield of acetaldehyde compared to that of silica. Since the activity of the catalyst depends on the number of active $B_2O_3$-crystallines, the role of alumina should be to stabilize the crystalline $B_2O_3$ on its surface. Moreover, alumina must generate and stabilize the cluster-type boron oxide, which is effective in the formation of acetaldehyde.

The authors wish to express their gratitude to Professor Koh-ichi Segawa and Mr. Du Soung Kim, Sophia University, for obtaining the XPS spectra.

**References**

1) E. M. Thorsteinson, T. P. Wilson, F. G. Young, and P. H. Kasai, *J. Catal.*, **52**, 116 (1978).
2) A. Argent and P. G. Harrison, *J. Chem. Soc., Chem. Commun.*, **1986**, 1058.
3) M. Iwamoto, T. Taga, and S. Kagawa, *Chem. Lett.*, **1982**, 1469.
4) L. Mendelovici and J. H. Lunsford, *J. Catal.*, **94**, 37 (1985).
5) K. Aika, M. Isobe, K. Kido, T. Moriyama, and T. Onishi, *J. Chem. Soc., Faraday Trans. 1*, **83**, 3139 (1987).
6) Y. Murakami, K. Otsuka, Y. Wada, and A. Morikawa, *Chem. Lett.*, **1989**, 535.
7) K. Otsuka and M. Hatano, *J. Catal.*, **108**, 252 (1987).
8) K. Otsuka, T. Komatsu, K. Jinno, Y. Uragami, and A. Morikawa, "Proc. 9th Int. Congr. Catal. (Calgary)," ed by M. J. Phillips and M. Terman, The Chemical Institute of Canada, Ottawa (1988), Vol. 2, pp. 915—922.
9) K. Komatsu, Y. Uragami, and K. Otsuka, *Chem. Lett.*, **1988**, 1903.
10) H. F. Liu, R. S. Liu, K. Y. Liew, R. E. Johnson, and J. H. Lunsford, *J. Am. Chem. Soc.*, **106**, 4117 (1984).
11) M. M. Khan and G. A. Somorjai, *J. Catal.*, **91**, 263 (1985).
12) S. Kasztelan and J. B. Moffat, *J. Catal.*, **106**, 512 (1987).
13) N. D. Spencer, *J. Catal.*, **109**, 187 (1988).
14) K. Marcinkowska, S. Kaliaguine, and P. C. Roberge, *J. Catal.*, **90**, 49 (1984).
15) F. N. Tavadze, V. V. Nemoshkalenko, D. L. Gabunia, A. I. Senkevich, T. Sh. Badzagua, G. A. Tsiskarishvili, and M. K. Tsomaia, *J. Less-Commun. Metal*, **117**, 135 (1986).
16) R. T. Pollard, "Comprehensive Chemical Kinetics," ed by C. H. Bamford and C. F. H. Tipper, Elsevier, New York (1977), Vol. 17, pp. 249—367.
17) R. W. Walker, "Reaction Kinetics," ed by P. G. Ashmore, Chemical Society, London (1975), Vol. 1, pp. 161—211.
18) A. N. Bashkirov, *Khim. Nauka i Prom.*, **1**, 273 (1956).
19) F. Broich and H. Grasemann, *Erdoel Kohle, Erdgas, Petrochem*, **18**, 360 (1965).